MICROSTRUCTURE, CREEP AND FRACTURE TOUGHNESS OF DIRECTIONALLY SOLIDIFIED NiAl/(Cr,Mo) ALLOYS MODIFIED WITH Hf, Si, Ta, Ti ADDITIONS

I. E. Locci*, S. V. Raj, J. D. Whittenberger**,**

J. A. Salem, D. Keller*****

[*]Case Western Reserve University at NASA Lewis Research Center, 21000 Brookpark Rd., MS 49-1, Cleveland, Ohio 44135, ilocci@lerc.nasa.gov

**NASA Lewis Research Center, 21000 Brookpark Rd., MS 49-1, Cleveland, Ohio 44135

[***]RealWorld Quality System Inc., Rocky River, Ohio 44116

ABSTRACT

A statistical design of experiments (DOE) strategy was implemented to optimize alloys based on the Ni-33Al-31Cr-3Mo eutectic system using small amounts of potential strengthening elements (Hf, Si, Ta, Ti). Following the analysis of the DOE results, several alloys were selected for directionally solidification (DS) utilizing a modified Bridgeman technique. The as-grown alloys were microstructurally examined by optical and scanning electron microscopy. They were also evaluated for fracture toughness at room temperature and compressive properties at 1300K. The microstructures and mechanical properties of these DS DOE alloys are discussed and compared to the directionally solidified Ni-33Al-31Cr-3Mo base composition.

INTRODUCTION

Significant improvements in the high temperature creep properties of NiAl alloys have been accomplished in the last decade [1-3]. Despite the success in creep behavior, the room temperature fracture toughness of most of these alloys is low. However, directionally solidified (DS) NiAl eutectic alloys, may offer a balance of properties that could enable the use of these alloys in aircraft engines. Directional solidification of NiAl alloys could produce in-situ composites, where the NiAl matrix and other phase(s) are aligned parallel to the growth direction [4-6]. Phases grown in this fashion are thermodynamically stable and tailored to play a critical role in the mechanical behavior response of the alloy. Desirable creep properties in the NiAl matrix might be enhanced by selecting the correct alloying additions, while the aligned second phase(s) create the potential for crack bridging and deflection that should enhance the overall toughness of the alloy. In this paper we examine the use of a design of experiments (DOE) strategy to select, process and evaluate the effectiveness of minor alloying additions to the Ni-33Al-31Cr-3Mo [5,7] eutectic system, where (Cr,Mo) is the reinforcing phase.

EXPERIMENTAL PROCEDURES

A statistical design of experiments (DOE) approach, summarized in Fig.1, was adopted in order to maximize the amount of the eutectic microstructure and to minimize the amount of primary dendrites and undesirable intercellular segregations. The benefits of any given DOE are that both simple and complex/interactive effects of several alloying elements are quantified reliably and efficiently (i.e. in a very minimum number of experiments). The design used was based on ternary additions that have demonstrated a positive effect on the strength of NiAl alloys [2]. The base composition was Ni-33Al-31Cr-3Mo (in at.%) [5,7]. The alloying elements investigated in the DOE were Al, Cr, Hf, Si, Ta, and Ti each at different levels/ranges. Mo was held fixed at 3 at.% and Ni was used as filler. The resultant DOE was comprised of 46 alloys including 5 repeats. Owing to the impracticality of directionally solidifying ~ 50 alloys, the as-cast microstructures of arc-melted castings were examined. It was assumed that the type of phases formed after arc melting and directionally solidification would be similar. All alloys were arc-melted and cast into rods 12.5 mm in diameter. Samples were sectioned in the mid-section of the cast rod, metallographically mounted and polished, and examined under optical and SEM conditions. After quantifying the results of the microstructural analyses in terms of % eutectic, % dendrite and % segregated phases, these data and alloy chemistries were subjected to statistical analyses where empirical models were built and then optimized to obtain the highest eutectic content. From these interactions, four alloys were chosen for directional solidification at a fixed withdrawal rate of 12.7 mm/h utilizing a modified Bridgeman technique. The directionally solidified region was typically about 19 mm in diameter and 100 mm long. The nominal and final chemical compositions after DS are presented in Table I.

DOE Methodology Used for Developing Directionally Solidified of Eutectic Alloys

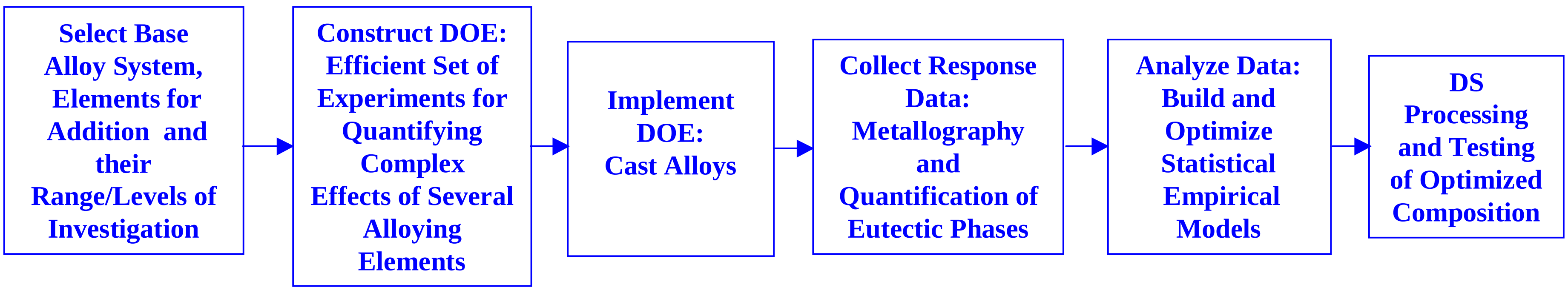

Figure 1

Table I: Nominal and Measured Chemical Composition of the DS alloys

Alloy Composition (at.%)

ID.	Ni	Al	Cr	Mo	Ta	Ti	HF	Si	O	C
AM-0 – Aim	33.0	33.0	31.0	3.0	------	-------	-------	-------	------	------
Actual	33.1	31.7	31.9	2.7	ND	ND	ND	ND	0.04	0.07
DK-1 – Aim	33.1	35.7	26.2	3.0	-----	0.06	1.50	0.20	------	------
Actual	32.8	36.0	26.9	2.9	ND	0.07	1.20	0.02	0.06	0.11
DK-10 - Aim	31.7	33.8	27.2	3.0	1.3	1.20	1.40	0.40	------	------
Actual	31.0	33.1	27.5	2.7	1.7	1.60	1.90	0.02	0.15	0.11
DK-10B - Aim	31.9	35.9	26.3	3.0	1.2	------	1.40	0.35	------	------
Actual	30.5	35.3	28.4	3.2	1.2	ND	1.20	ND	0.12	0.09
DK-10C - Aim	32.6	34.7	27.2	3.0	1.3	1.20	------	------	------	------
Actual	30.7	34.0	29.3	3.1	1.4	1.30	ND	ND	0.05	0.08

ND – Not detected

EXPERIMENTAL PROCEDURES (Cont.)

For creep testing, nominally 5 mm diameter by ~10 mm long cylindrical compression specimens were wire electro-discharge machined (EDM) from the as-grown bars with sample length parallel to the growth axis. Compressive stress - strain behavior at engineering strain rates ranging from about 2 x 10^{-4} s^{-1} to 2 x 10^{-7} s^{-1} were measured in air at 1300K under constant crosshead velocity conditions in a universal test machine. A few samples were also tested in air at 1300K under constant load compressive creep conditions in lever arm test machines.

Fracture toughness of the alloys was measured using a chevron-notch flexure specimen in accordance with ASTM test method PS070 for ceramics [8]. Four test specimens per alloy, measuring about 3 mm in thickness and 6 mm in width, were loaded at a stroke rate of 0.05 mm/min between 20 and 40 mm spans (i.e. configuration "C" of PS070). The specimen stability was monitored by either placing a strain gage on the specimen compressive [9] face or with an extensometer contacting the load train. Both methods were adequate for assessing the crack stability.

RESULTS AND DISCUSSION

Microstructure

Typical back-scattered electron (BSE) micrographs of the arc-melted alloys from DOE are presented in Fig. 2. The alloys were comprised of up to 4 different microstructural features: a 2-phase eutectic region with lamellae of the NiAl phase and (Cr,Mo) phase; a 3-phase eutectic consisting of the previous two phases and (based on energy dispersive spectroscopy,EDS, and X-ray diffraction) a Laves phase (i.e. Cr_2Ta); NiAl dendrites; and intercellular phases. The statistical empirical models built were used to optimize the total amount of eutectic phases (2 + 3 phase eutectic). From these interactions, four alloys (listed in Table I) with a volume fraction > 90% eutectic (2 + 3 phase eutectic) and the base composition were selected for DS.

Back-scattered electron images of arc-melted DK Alloys.

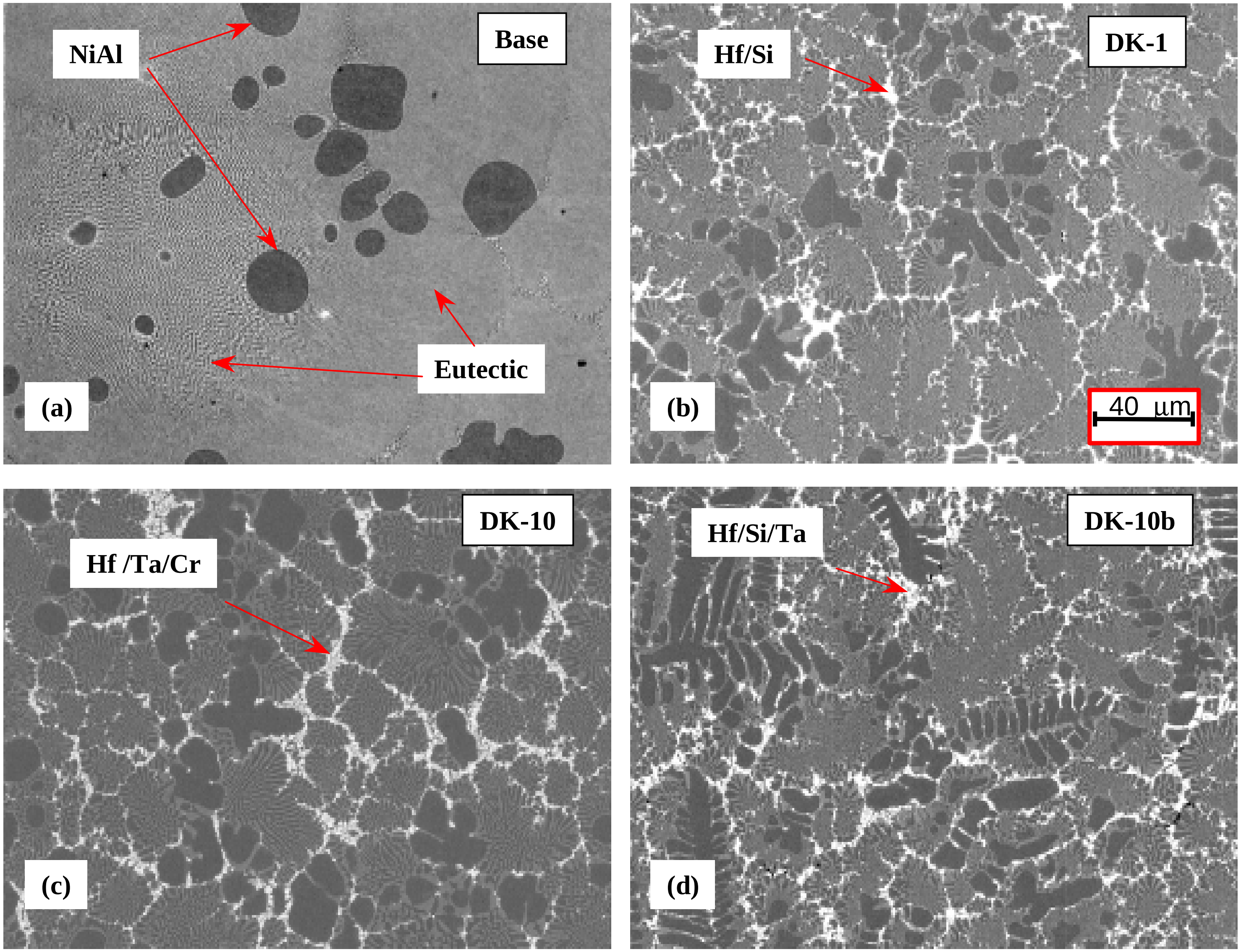

Figure 2

Microstructure (cont.)

The microstructure of the base composition (Fig. 3a) did show a clear preferential orientation due to the DS process, although some growth faults disrupting the lamellar DS microstructure were observed. Figure 3b shows the longitudinal microstructure of the DK-1, DK-10, DK-10B and DK-10C alloys observed after DS. Coarser microstructures, and a reduction on the degree of alignment was significant in the DS DK alloys compared to the base alloy; however the intercellular segregation that was seen in the arc-melted condition was reduced (Fig. 3b). EDS analyses (Fig. 3c), of both arc-melted and DS samples, show that the ternary additions (Hf, Ta, and Si) had a tendency to segregate intercellularly (white region) with a smaller detectable amount of Cr and Mo. Titanium had a tendency to partition mostly to the NiAl phase. Alloys DK-1 and DK-10B showed even less alignment than DK-10.

Back-scattered electron image of the base composition 33Ni-33Al-31Cr-3Mo

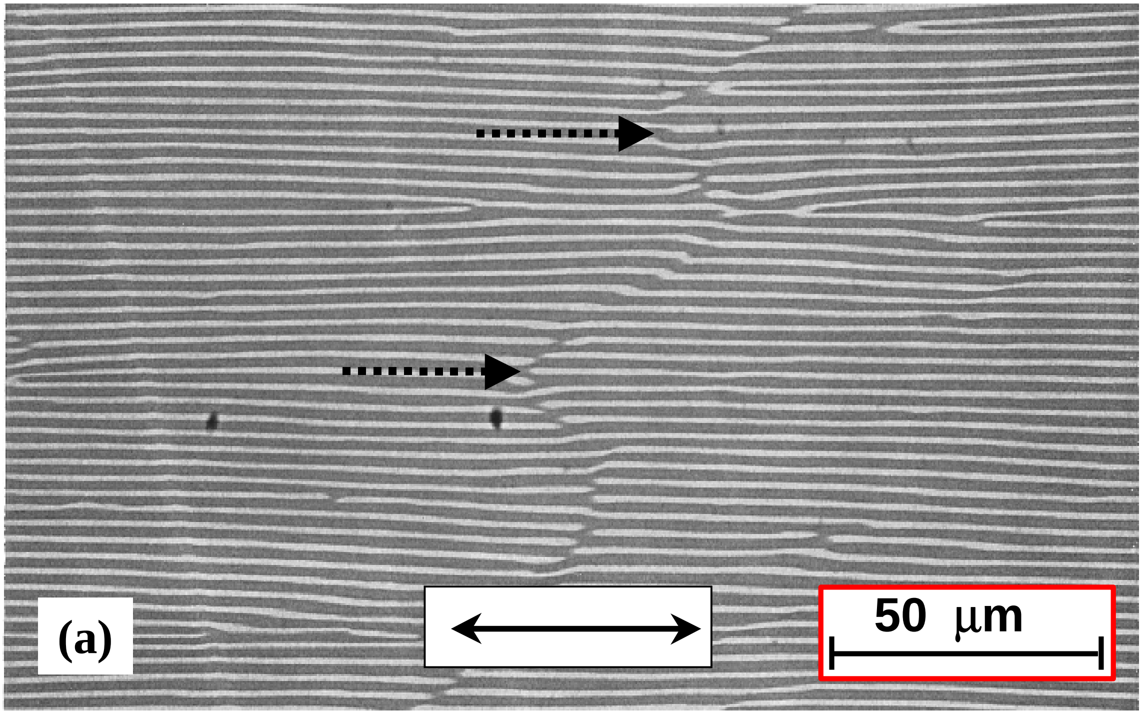

Solid arrow denote the withdrawal direction
Broken arrows indicate growth faults

Figure 3 (a)

Back-scattered electron images of longitudinal sections of the directionally solidified DK alloys.

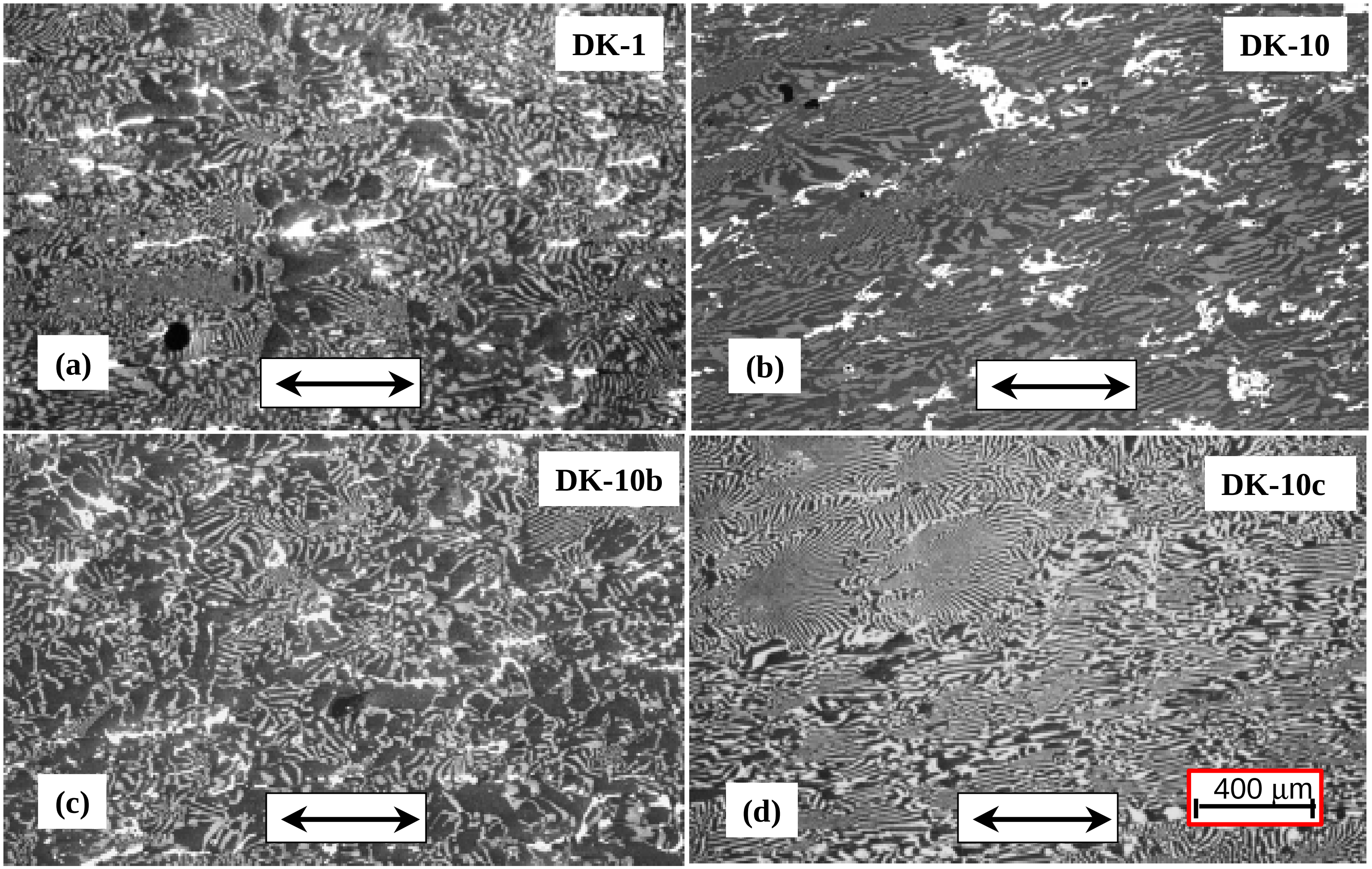

The arrows denote the withdrawal direction.

Figure 3(b)

Typical Element Distribution Observed in the DS alloy DK-10C

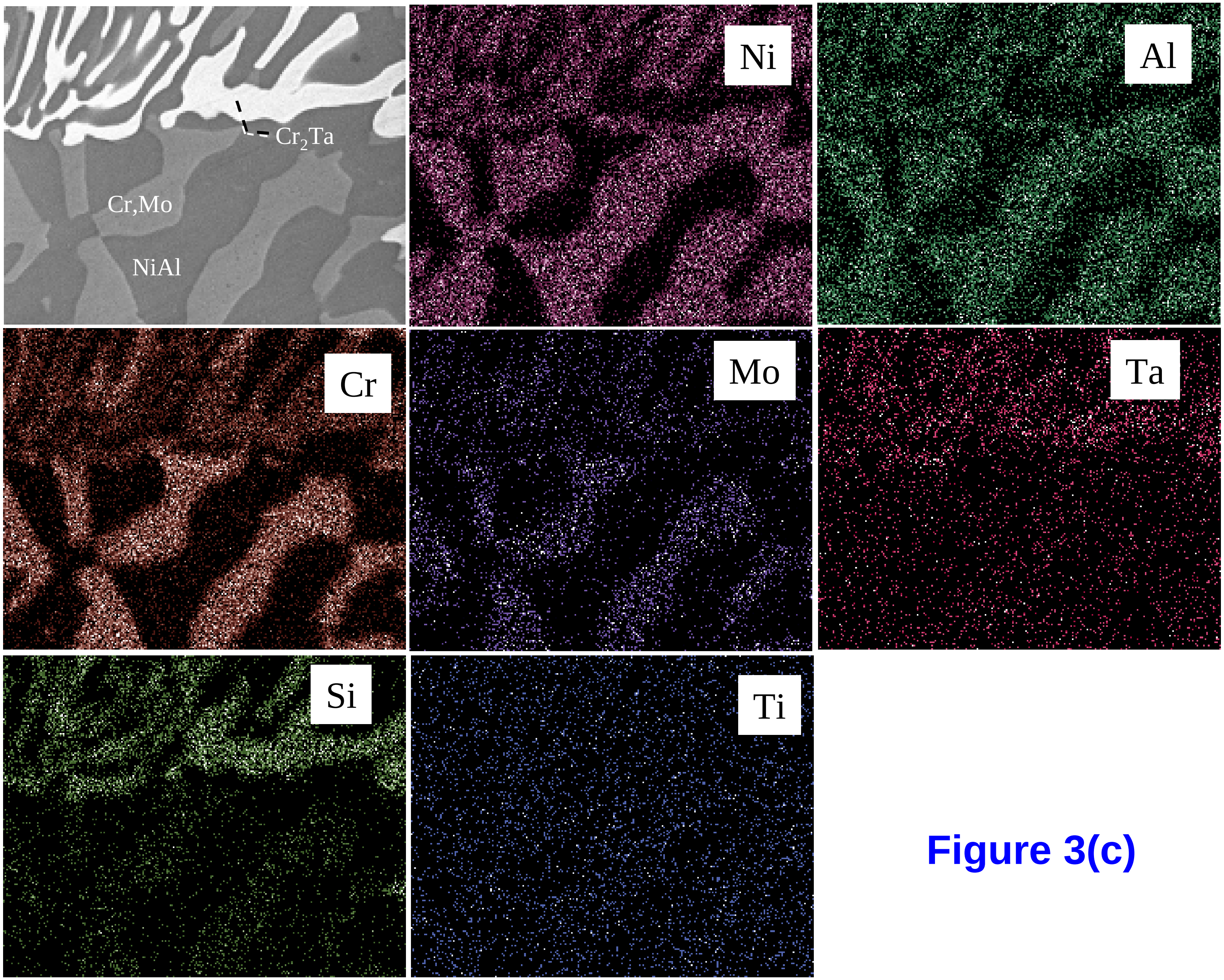

Figure 3(c)

DOE Predictions and Observations

Table II shows the percentage of predicted and observed volume fraction of eutectic phase(s) for the base composition alloy and the DK series of alloys. The microstructures of the DK alloys had lower than expected amounts of eutectic, including a total absence of the 3-phase eutectic. Much of this discrepancy can be traced to slight differences between the aim and actual chemistries. When the actual compositions are used, the predictions of the DOE models are improved, but are still only approximate. It is believed that accuracy of the models is limited by the large amount of intercellular phases that affected the response data (i.e. % eutectic, % dendrites, etc.).

Table II. DOE Prediction and Microstructural Observation of the Eutectic Phase

Alloy Designation	Predicted Vol. (%) Eutectic Using Aim Compositions 2-phase / (3-phase)	Predicted Vol. (%) Eutectic Using Actual Compositions 2-phase / (3-phase)	Observed Vol. (%) Eutectic 2-phase / (3-phase) After Arc melting
Base	86 / (0)	86 / (0)	92 / (0)
DK-1	94 / (0)	89 / (0)	73 / (0)
DK-10	72 / (23)	68 / (0)	73 / (0)
DK-10B	80 / (20)	76 / (0)	55 / (0)
DK-10C	74 / (22)	65 / (1)	90 / (0)**

** Examined in DS condition

1300K COMPRESSIVE TESTING

Typical examples of the true stress – true strain curves for the four DK alloys determined at 1300K for two constant engineering strain rates are shown in Fig. 4(a). At $\sim 2 \times 10^{-7}\ s^{-1}$, all materials display similar behavior and strength levels, where plastic flow occurred at a more or less constant stress after minor strain hardening. At an imposed strain rate of $\sim 2 \times 10^{-5}\ s^{-1}$, alloy DK-10 demonstrated extensive strain hardening over about 4 % deformation to a maximum stress of approximately 260 MPa; the other three alloys exhibited work hardening only over the first 1 % strain leading to maximum stresses between 205 and 235 MPa. After reaching their maximum stresses at $\sim 2 \times 10^{-5}\ s^{-1}$, all four DK materials underwent gradual strain softening. Only two alloys were compression creep tested at 50 MPa and the resulting curves are presented in Fig. 4(b). Both tests displayed well-defined normal primary and secondary creep regimes with measured steady-state creep rates being within a factor of two: $9.6 \times 10^{-9}\ s^{-1}$ (DK-10B) and $1.6 \times 10^{-8}\ s^{-1}$ (DK-10C).

Compressive behavior of the DK series of alloys at 1300 K

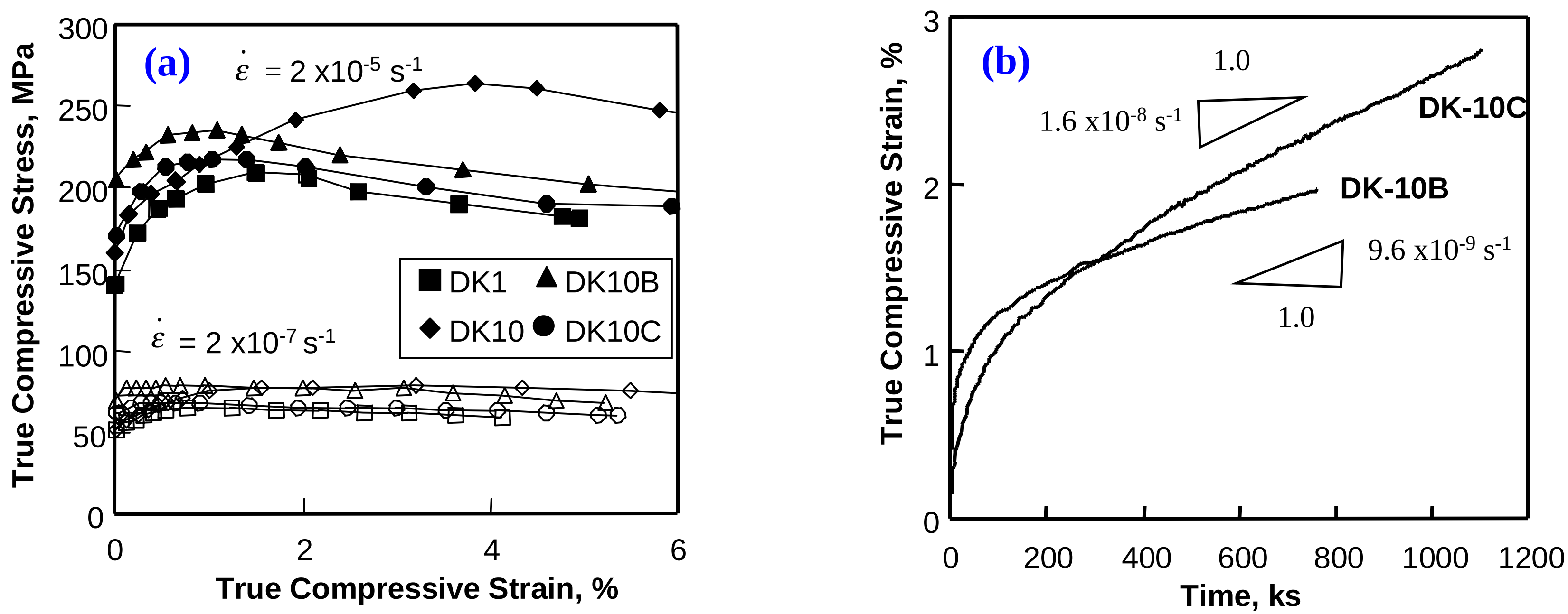

(a) True stress – strain curves determined by constant velocity testing
(b) Creep curves for an engineering stress of 50 MPa.

Figure 4

1300K COMPRESSIVE TESTING (cont.)

The true compressive flow stress – strain rate behavior for the DK series is illustrated in Fig. 5(a), where flow stresses and strain rates from the constant velocity tests (Fig. 4a, open symbols) were evaluated at 1 % strain, while the steady state values from the two constant load creep tests (Fig. 4b, filled symbols) were utilized. No significant difference in strength exists among the four alloys; hence, all the data were joined and fitted to a power law expression:

$$\dot{\varepsilon} = 1.82 \times 10^{-15}\, \sigma^{4.26}\ \mathrm{s}^{-1} \qquad (1)$$

where the coefficient of determination is 0.96 and the standard deviation of the stress exponent is 0.23. The result of this fit is shown in Fig. 5(a) as a straight line, which characterizes the data well. The 1300K strength of the directionally solidified DK series of alloys is compared in Fig. 5(b) to that of NiAl [001] single crystals [10] and directionally solidified base alloy 33Ni-33Al-31Cr-3Mo. This figure reveals that properties of the DK alloys are significantly better than binary NiAl; unfortunately they are not improved in comparison to the base alloy.

Compressive flow behavior of directionally solidified NiAl-based alloys at 1300 K

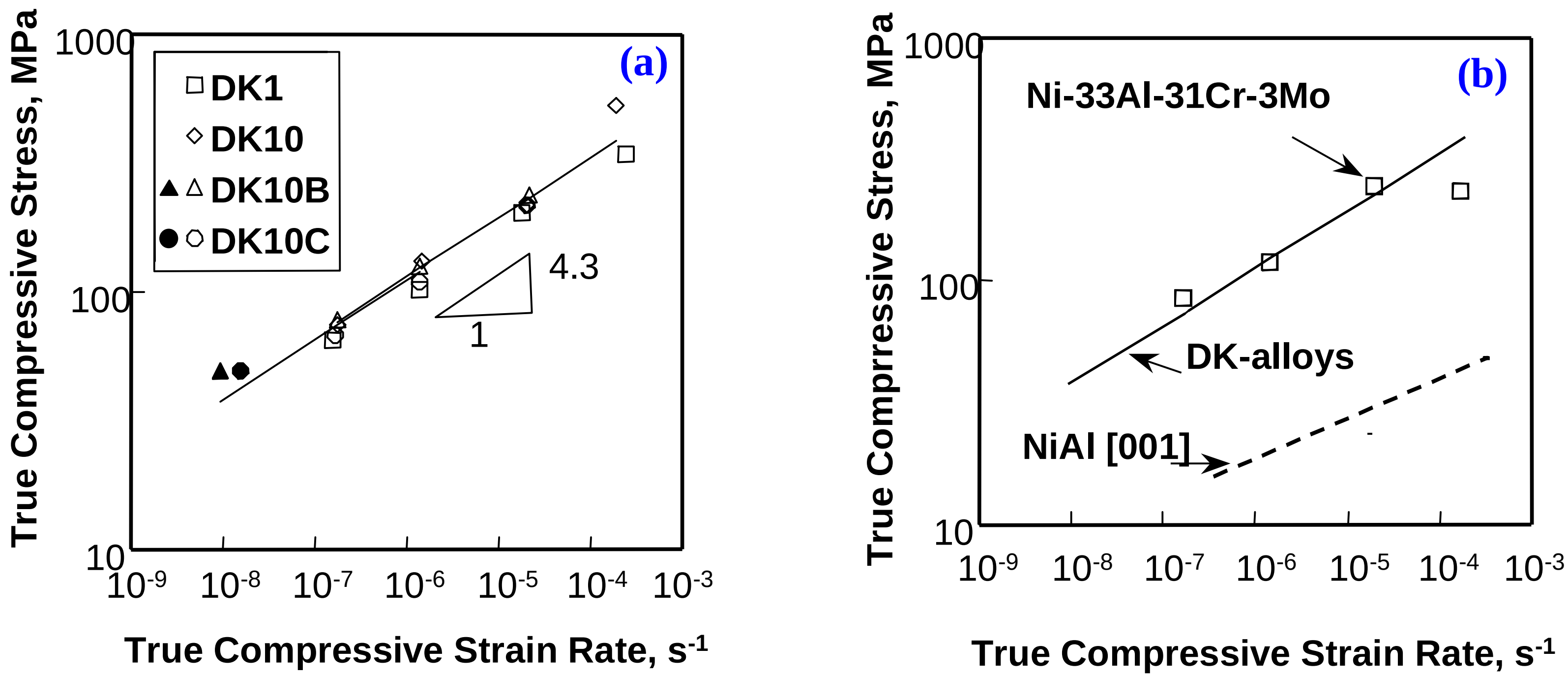

(a) DK series of alloys.
(b) comparison of DK series and Ni-33Al-31Cr-3Mo with NiAl [001] single crystals.

Figure 5

FRACTURE TOUGHNESS

During toughness testing, the majority of the specimens exhibited multiple, unstable crack extensions followed by crack arrests instead of the stable extension required for valid results. In order to estimate fracture toughness values from the specimens exhibiting crack jumps, the specimen compliance, as estimated from the load-displacement diagrams, were used to estimate crack lengths and directly calculate a fracture toughness associated with each crack jump. Comparison of the fracture toughness estimated from compliance and from the maximum load, in accordance with PS070, gave similar results: 11.3 vs. 11.5 MPa√m for a specimen of the base alloy. The data (average and standard deviation) are summarized in Table III. The DK alloys are particularly brittle, with a fracture toughness of ~5 MPa√m, while the base alloy is substantially tougher, with an estimated fracture toughness of ~12 MPa√m. The fracture surfaces of two specimens from the base alloy, one with a low toughness and one with a more typical higher fracture toughness are compared in Fig. 6. Note that the lamellae in Fig. 6(a) are nearly parallel to the macroscopic crack growth direction in the low toughness specimen. Fig. 7(a) shows unstable crack initiation in a DK-10C specimen from a chevron tip, and Fig. 7(b) shows unstable crack initiation in a DK-10 specimen from a large second phase particle located on the side of the chevron near the tip. The coarser microstructure observed in the DK alloys, and the resultant unstable crack extension imply that larger specimens or a different technique should be considered in order to obtain valid K_{Ic} measurements. Nevertheless, these fracture toughness values represent upper bounds and indicate the need for more refined and uniform microstructures. This may not be achievable for the chosen alloy additions.

Table III - Estimated FractureToughness of the Alloys.

Alloy Designation	Fracture Toughness MPa$\sqrt{m}$
Base	12.0 ± 1.7
DK-1	5.4 ± 0.1
DK-10	4.8 ± 0.1
DK-10C	5.8 ± 0.1

Chevron notch flexure (vb) specimen

(standard proportions and tolerances)

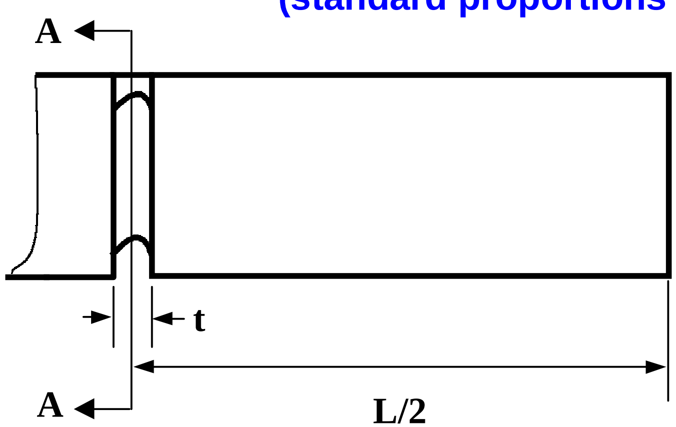

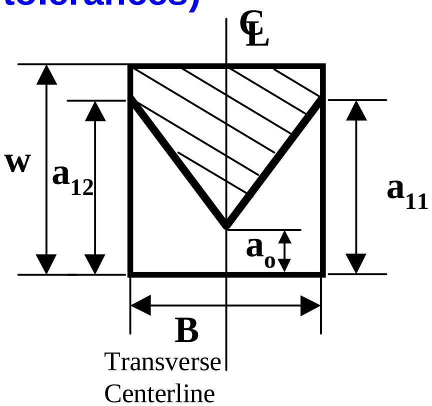

Section A-A

Configuration and test fixture	L (mm)	B (mm)	W (mm)	a_o (mm)	a_{11} and a_{12} (mm)	t (mm)
C (Four-point)	45 (min)	3.00 ± 0.13	6.00 ± 0.13	1.20 ± 0.07 (no overcut)	4.20 ± 0.07 (no overcut)	<0.25

Back-scattered scanning electron microscope images of the fracture surfaces of Ni-33Al- 31Cr-3Mo

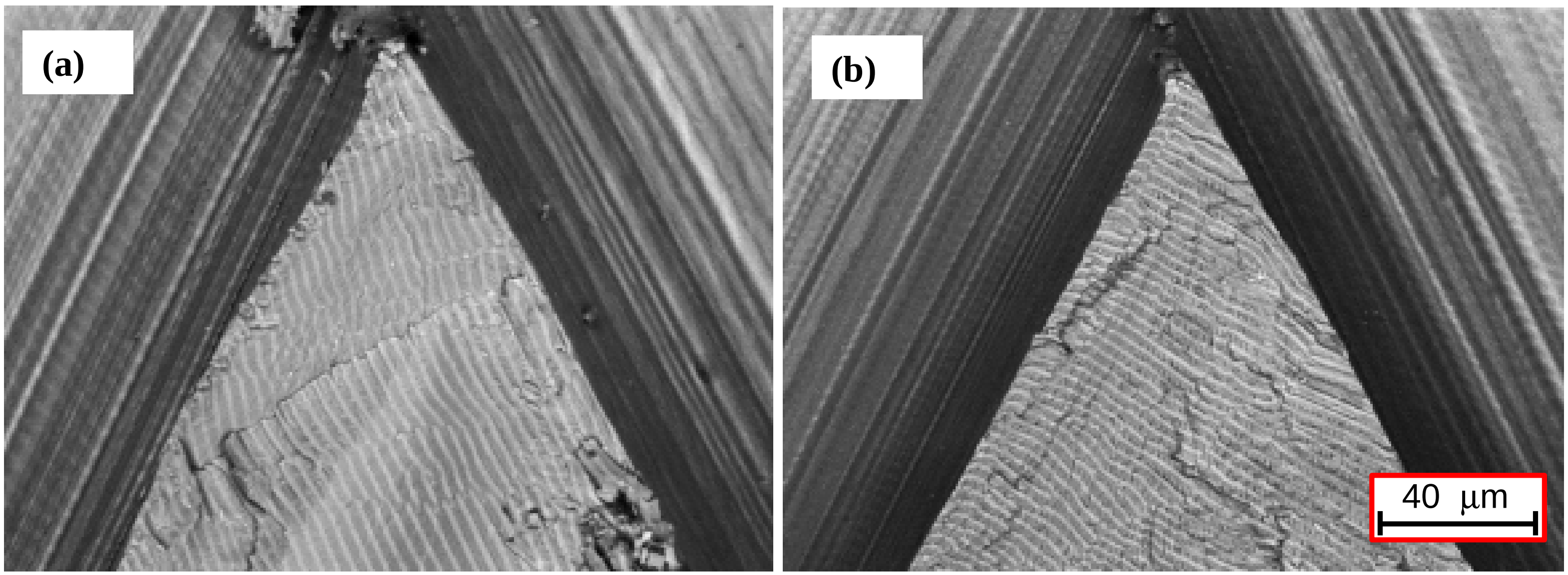

K_{Ivb}=6.1 MPa√m

K_{Ivb}=12 MPa√m

Figure 6

Secondary and back-scattered images of the fracture surface of alloy DK-10C

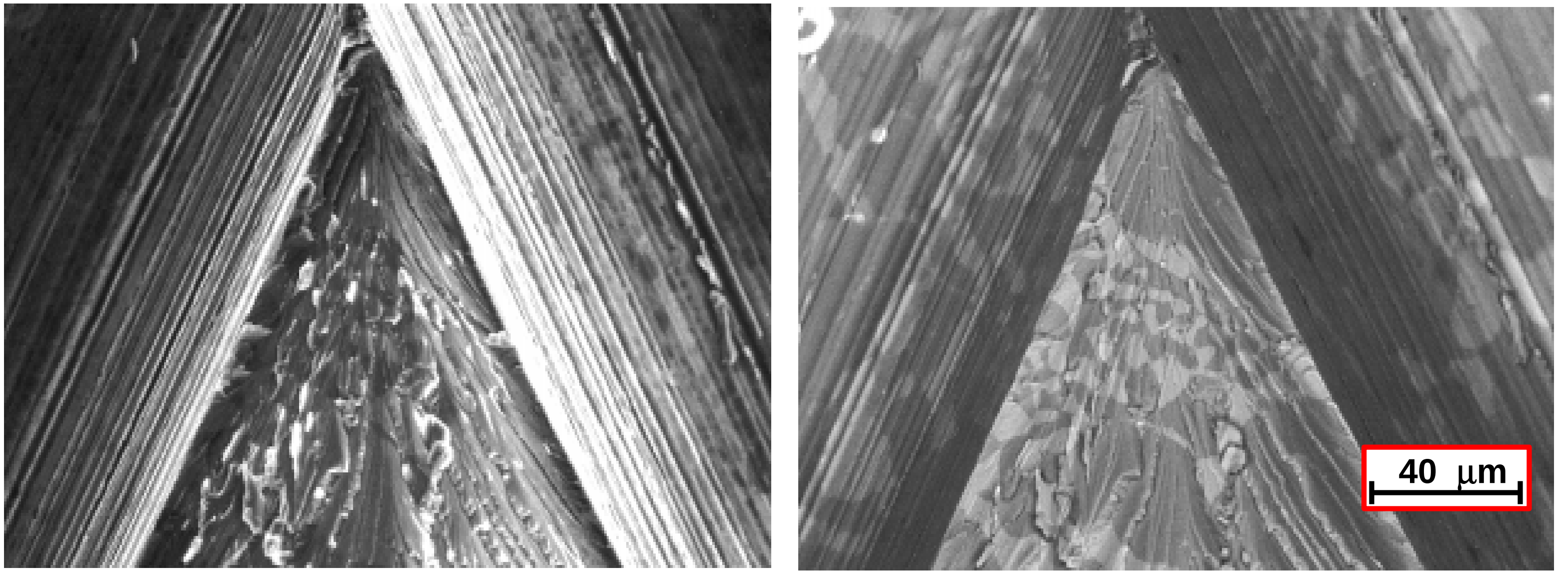

Secondary electron Image Back scattered electron image

K_{Ivb}=4.8 MPa$\sqrt{}$m.

Figure 7(a)

Secondary and back-scattered images of the fracture surface of alloy DK-10

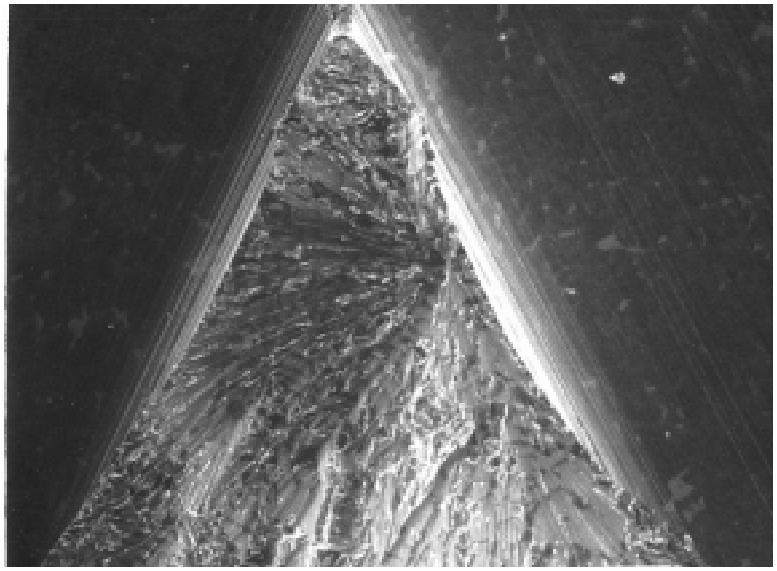

Secondary Electron Image

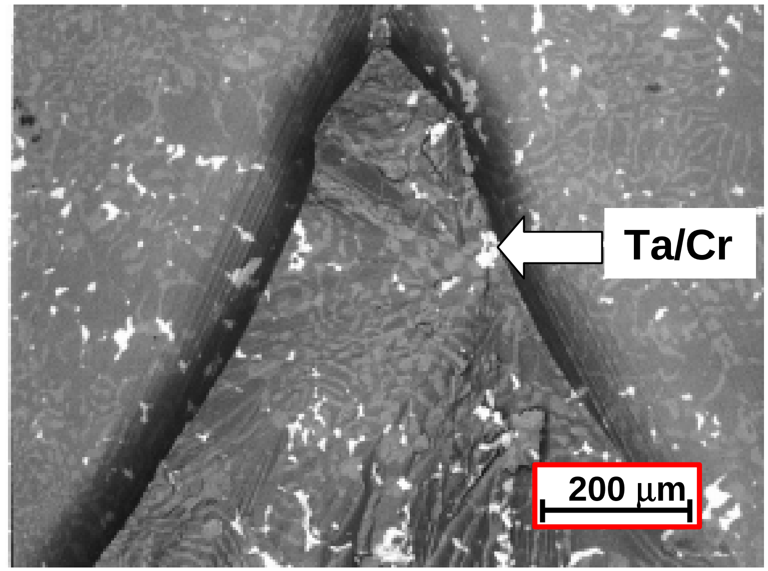

Back-scattered Electron image

K_{Ivb}=5.4 MPa$\sqrt{}$m.

Figure 7(b)

SUMMARY AND CONCLUSIONS

Directionally solidified alloys based on Ni-33Al-31Cr-3Mo with additions of Hf, Si, Ta, and Ti, were evaluated as potential candidates for turbine engine applications. A DOE approach based on arc-melted buttons was used to select four alloys for DS processing and subsequent creep and fracture toughness testing. The downselected alloys did not contain the desired microstructures, due to both the limited accuracy of the DOE models, plus sensitivity to small deviations from the aim chemistries. Compared to the baseline eutectic alloy, all of the complex alloys exhibited reduced fracture toughness combined with no improvements in creep strength. Although improvements in microstructure through processing refinements plus tighter composition control are avenues for improved properties, the present study underscores the difficulty in DS eutectic alloy design. The desire to add significant levels of alloying additions in order to impart significant strengthening appears to be compromised by the tendency for these same levels of alloying to inhibit the formation of fine eutectic microstructures.

REFERENCES

1. J. D. Whittenberger, E.Artz and M. J. Lutton, J. Mat. Res., **5**, 271-277, (1990).
2. M. V. Nathal, in *Ordered Intermetallics – Physical and Mechanical Behavior*, C.T. Liu, R. W. Cahn and G. Sauthoff, eds. (Kluwer Academic Publishers, Dordrecht, The Netherlands, 1992), pp. 541-563.
3. R. Darolia and W. S. Walston, in *Structural Intermetallics-1997*, M.V. Nathal, R. Darolia**,** C. T. Liu, P. L. Martin, D. B. Miracle, R. Wagner and M. Yamaguchi, eds. (The Minerals, Metals, & Materials Society, Warrendale PA, 1997), pp. 585-594.
4. J. L. Walter and H. E. Cline, Metall. Trans., **1**, 1221-1229 (1970).
5. H. E. Cline and J. L. Walter, Metall. Trans., **1,** 2907-2917 (1970).
6. J. M. Yang, JOM, **49** (8), 40-43 (1997).
7. D.R. Johnson, X. F. Chen, B. F. Oliver, R. D. Noebe and J. D. Whittenberger, Intermetallics, **3**, 99-113 (1995)
8. "Standard Test Method for Fracture Toughness of Advanced Ceramics," Test Method PS070, American Society for Testing Materials Annual Book of Standards, 15.01 ASTM, West Conshohocken, PA, 1998.
9. J.A. Salem, L.J. Ghosn, and M.G. Jenkins, *Ceramic Engineering and Science Proceedings*, Vol. 19, Issue 3-4, 1998, in print.
10. J. D. Whittenberger, I. E. Locci, R. Darolia. Submitted to Mater. Sci. Eng.